Correlation between Retinal Ganglion Cell Loss and Nerve Crush Force-Impulse Established with an Instrumented Tweezers in Mice

Xiaorong Liu[1, 2, 3 †], Liang Feng[1], Ishan Shinde[4], James D. Cole[3], John B. Troy[5], and Laxman Saggere[4, †]

1. Department of Ophthalmology, Northwestern University, Evanston, IL;

2. Departments of Biology and Psychology, University of Virginia, Charlottesville, VA;

3. Neuroscience Graduate Program, University of Virginia, Charlottesville, VA;

4. Mechanical and Industrial Engineering, University of Illinois at Chicago, Chicago, IL;

5. Department of Biomedical Engineering, Northwestern University, Evanston, IL.

[†] Corresponding authors:

Xiaorong Liu, xl8n@virginia.edu

Laxman Saggere, saggere@uic.edu

ARVO poster presentation 2019

Abstract

Purpose: Rodent models of optic nerve crush have often been used to study degeneration and regeneration of retinal ganglion cells (RGCs) and their axons as well as the underlying molecular mechanisms. However, optic nerve crush results from different laboratories exhibit a diverse range of RGC damage lacking consistency, reliability and a means for quantification of the degree of axonal damage. Therefore, in this study, we examined the correlation between RGC axon loss and impulse, the product of force and duration, applied through self-closing Dumont tweezers to crush optic nerves.

Methods: We instrumented a pair of standard self-closing #N7 tweezers with miniature foil strain gauges at optimal locations on both arms of the tweezers. The instrumented tweezers was capable of recording the tip closure forces in the form of voltages, which were calibrated through load cells to corresponding tip closure forces over the operating range. Using the instrumented tweezers, we crushed the optic nerves of multiple mice with varied forces and durations and the crushed optic nerves were dissected and prepared for immunostaining for axon counting.

Results: We plotted surviving axon density versus the corresponding crush force impulse. We found that the surviving axon density correlated with crush force, with longer duration and stronger crush forces producing consistently more axon damage.

Conclusions: A simple and repeatable technique for measurement of optic nerve crush forces in real-time is introduced here for the first time. Using the instrumented tweezers presented in this

study, experimenters can be trained to apply controlled forces during optic nerve crush to produce consistent and predictable post-crush cell death. This should permit future studies a way to produce nerve damage more reliably than is available now.

Layman Abstract:

We examined the relationship between the force delivered to the optic nerve and neuron damage in mice. Our long-term goal is to design a new instrument to deliver consistent damage to the optic nerve with controlled force, duration, and location, so that one can study neuron loss and its underlying mechanisms in a controlled manner.

Introduction

Rodent models of optic nerve crush (ONC) have often been used to study degeneration and regeneration of retinal ganglion cells (RGCs) and the underlying molecular mechanisms (Duan et al. 2015, Fischer et al. 2017, Kalesnykas et al. 2012, Oglesby et al. 2012, Quigley 2016, Quigley et al. 1981). For example, RGC death may be triggered by different signaling paths in different forms of glaucoma, so experimental models have been developed to mimic these different forms. Although an experimental ONC injury may not be a "true" model of glaucoma, it represents an optic neuropathy leading to acute RGC death that is often assumed to involve some of the same molecular mechanisms as those responsible for RGC death in types of glaucoma. Moreover, rodent models of ONC offer the advantage of producing a rapid and profound loss of RGCs that expedite investigations of mammalian mechanisms of neural regeneration (Howell et al. 2007, Howell et al. 2008, Nickells et al. 2012).

However, a major drawback with current rodent models of ONC is that the degree of RGC loss for each crush trial varies substantially from laboratory to laboratory and, within a laboratory, from investigator to investigator. Results from crush experiments conducted in different laboratories exhibit a diverse range of RGC damage, lacking consistency, reliability and a foundation for quantifying the degree of axonal damage (Table 1). For example, at 2-weeks (w) following optic nerve crush, Leung and his colleagues report about 89% RGC loss (Leung et al. 2008), while Sharma and her colleagues report just 30% RGC loss (Sharma et al. 2014), and Li and Nickels report 58% RGC loss at 3-w post injury (Li et al. 1999). The extent to which these differences can be ascribed to variation between laboratories and variation between individuals performing the crush is unclear, although RGC or axon loss is likely relatively consistent within

each laboratory when one person performs the crush; e.g., individuals from our laboratory achieve less than 10% variation in RGC loss from experiment to experiment (Puyang et al. 2016).

The inter-laboratory variability in ONC models could be reduced if a standard calibrated tool for crushing were available. The common crush technique (pinching the nerve with a tool for 2-3 seconds) and the resulting damage rely on manual actuation of the tool and operator characteristics of holding the tool during an ONC trial. Obviously, this approach is subject to great variation from investigator to investigator as discussed above (also see Table 1). As a result, the spatial patterns of the axonal damage vary greatly, making comparison between different groups difficult.

In this study, we examined how varied duration and force together affected RGC survival in the optic nerve crush injury in mice using instrumented tweezers with the objective of identifying a means to control nerve injury.

Methods

Development of Instrumented Tweezers

First, the range of mechanical strains experienced by the tweezers during its normal range of operation was analyzed via Finite Element Analysis in COMSOL Multiphysics software, where the exact geometry of the tweezers including their curved tips (0.03×0.07 mm^2), obtained through imaging, and the tweezers' material properties, assumed to be INOX stainless steel with the Young's modulus of 200 GPa, were represented. Based on the simulation and analysis of the mechanics of the tweezers, the mechanical strain was found to range from 0 to 10^{-4} corresponding to a maximum tip displacement of 5.4 mm, with the maximum strain located at a point approximately 16 mm from the base of the tweezers.

We evaluated several different types of sensors including foil strain gauges, piezoelectric sensors, polyvinylidene fluoride thin films, optical fiber Bragg grating and custom MEMS-based sensors weighed against the desirable sensor characteristics; the commercially available miniature precision foil strain gauge (SGD-3/120-LY11, Omega Engineering, USA) with an overall footprint of 3 mm × 3.8 mm was found to be best suited for integration with the tweezers in this study.

Two miniature precision foil strain gauges were mounted on the #N7 tweezers, one on each arm centered 16 mm from the base of the tweezers for maximum signal sensitivity and packaged using Parafilm M® to provide electrical insulation and water resistance and mechanical protection. The leads from each strain gauge were soldered to 32 AWG wires and encapsulated in a heat shrink tube for safety and portability. The other ends of the lead wires were connected

to a data acquisition (DAQ) system using a three wire quarter bridge configuration via push-in connectors (Figure 1). The DAQ system comprised of a bridge completion module, a voltage source and an analog-to-digital DAQ board (USB-6212 BNC, National Instruments Corp., USA), with the strain gauge data acquired by LabVIEW software.

The compressive forces for various openings of the tweezers tips were calibrated to the strain gauge voltage signals by placing a subminiature load cell with 1000 g load range (Model 13, Honeywell Inc., USA) between the tips of the tweezers and recording both the voltage signals from the strain gauges. The force output of the load cell for tweezers' tip openings were ranging from 3.3 mm (the thickness of the load cell) to 5.5 mm in increments of 0.25 mm, and the data were extrapolated down for tip openings below 3.3 mm. The resulting voltage vs strain (crush force) relationship was found to be linear for the self-closing tweezers' openings (grasped object sizes) up to 5.5 mm.

Optic Nerve Crush Injury and Axon Counting

Mice were anesthetized through intraperitoneal injection of ketamine (100 mg/kg) as described previously (Puyang et al. 2016, Puyang et al. 2017). In brief, small cuts were made in the superior and lateral conjunctiva to expose the optic nerve. The optic nerves were crushed with the instrumented #N7 reverse grip tweezers at a distance between 0.5 and 1 mm from the globe. Both the intensity of the crush force applied and the duration of applied force in each trial were recorded through the data acquisition system connected to the instrumented tweezers. In each crush trial, the strain gauges were first normalized and their initial readings were reset to zero, and then, strain output signals from the instrumented tweezers were continuously acquired

by the DAQ system from the moment the operator grasped the optic nerve between the tweezers' tips until the optic nerve was released from the tweezers' grasp. The duration of crush was varied between 2 to 9 seconds, which are common times used by various laboratories. Finally, the strain recordings recorded in the form of voltages were scaled to corresponding crush forces, according to the calibration.

Mice were sacrificed at one or three days following crush, and their optic nerves dissected, cryo-sectioned, and immunostained for axon counting. Cryo-Sections (14-18um thick) were taken between 0.5 and 1 mm from the ONH and stained using P-phenylenediamine (PPD 1:50, Fisher). The stained sections were then imaged using a Zeiss Observer A1 microscope (Carl-Zeiss, Oberkochen, Germany) and a total of 20 images covering the center, mid-periphery, and peripheral margin of each optic nerve were recorded. The axons in each of the three regions of the optic nerve were counted using Imaris software (Bitplane, Concord, MA). Counts were averaged and normalized with respect to the area of the region of optic nerve studied to obtain axon density (Chen et al. 2015).

Results

We determined the range of mechanical strains experienced by the tweezers during its normal range of operation by Finite Element Analyses, and then selected the miniature precision foil strain gauge (SGD-3/120-LY11, Omega Engineering, USA) mounted on the #N7 tweezers (Figure 1). When an object is held between the tips of the tweezers, the strain gauges mounted on the tweezers' arms transduce the compressive force applied by the tweezers on the object into voltage signals. Following the calibration as described in the Methods, the experimenter was trained to maneuver and actuate the tweezers expertly. Next, crush forces were applied for various amounts of time using the feedback of signals from the strain gauges to examine RGC survival following crush injury.

As shown in Figure 2, optic nerve crush produces known signs of axon degeneration and loss (Chen et al. 2015, Howell et al. 2007, May & Lutjen-Drecoll 2002). At 1-day post optic nerve crush injury, there was a significant loss of axon density (Figure 2). In control mice, individual axons (dark PPD stained circles) appear normal and tightly packed, while crushed optic nerves have fewer axons per section. Additionally, the sections reveal other signs of degeneration, most notably the accumulation of vacuoles amongst dead or dying axons (orange arrow), axonal swelling (green arrows), and the abundance of degenerative debris in the form of dystrophic neurites (blue arrows, Figure 2).

Our results indicate that prolonged crush duration and increased force results in greater axon degeneration. To study the combined effects of the crush duration and the crush force, we plotted axon density against the crush force impulse (newton-second), which revealed that axon density declines with increased force impulse (Figure 3). This relationship is represented with a

consistent and predictable power trend line (R^2= 0.77), reaching an asymptotic density as force-impulse approaches 8 newton-second.

To demonstrate that crush duration and force intensity were uncorrelated in our experiments, we plotted the duration *versus* intensity data (Figure 4). Strong or weak crush force was delivered each time randomly which showed no correlation with duration. With the instrumented self-closure tweezers, we sought to provide a consistent force delivered by one investigator. In crushes with longer duration (> 20 seconds), the crush force stabilized around 0.25-0.30 N. Using feedback from the sensors' readings, the experimenter could learn to deliver more or less consistent force around 0.3 N. Together, our data suggest that the experimenter can be trained to deliver controlled forces for the optic nerve crush injury.

Discussion

In this study, we sought to measure the ONC forces in-situ in real time and examine, for the first time, how crush duration and crush force affect RGC survival in ONC trials in mice by sensorizing Dumont #N7 self-closing tweezers. Historically, a variety of tools and methods including silk threads, needles, glass rods, clamps, aneurism clips, special cuffs, custom micro-injuring devices and different types of forceps have been used by groups seeking to study the impact or severity of the ONC (Burke et al. 1985, Cottee et al. 1991, Gellrich et al. 2002, Klocker et al. 2001). For example, Cottee et al.. used a deflated balloon fastened inside a brass cylinder, which was hooked around the optic nerve via an extensive surgical procedure (Cottee et al. 1991). The balloon was inflated to squeeze the optic nerve and completion of the crush imparted was indicated by a block of optic nerve conduction. The estimated pressure required to cause the ONC ranged widely from 70 kPa to 200 kPa (Cottee et al. 1991). Gellrich and co-investigators used a micro-hook Newton Meter Dynamometer-micromanipulator assembly to deliver graded crush forces to the optic nerve and reported the crush forces to be in the range of 0.05 N to 0.2 N (Gellrich et al. 2002, Klocker et al. 2001). However, this being a non-standard tool, the size and topology of its tip or area of contact with the optic nerve unreported, the results are difficult to interpret. Factory calibrated aneurism clips and other surgical clips delivering crush forces in the range 0.58 N to 1.82 N have been used to perform ONC (Feng et al. 2010, Maeda et al. 2004, Sarikcioglu et al. 2007, Tsai et al. 2008), but these clips are not well suited for ONC as their closing forces cannot be controlled and they are difficult to operate, and require lateral canthotomy surgery to access the optic nerve.

As shown in Table 1, one of the oldest and most common tools employed for ONC are surgical tweezers. The majority used have a cross-action type design, like the one used in our

study here. This design ensures a self-closing action and application of a constant crush force over the crush duration. For example, several groups used Dumont #N5 (Li et al. 1999, Li et al. 2007, Tang et al. 2015) or #N7 (Templeton 2012) cross-action tweezers to study the effects of ONC, although in none of these studies was the intensity of crush noted. More recently, Huang and coworkers used a cross action tweezers to perform ONC and calibrated them using a lever arm approach, where weights were added to the tweezer arm tips to measure the closing force (Huang et al. 2015). They, however, did not investigate the effect of crush duration as we have which we found to affect axon loss also. In our study, for the first time, we quantified the relationship between crush intensity (product of force and duration in the operational range) and the severity of injury measured as axonal loss post crush.

In summary, we investigated the combined effects of crush parameters measured in real time on RGC survival after optic nerve injury in mice. With calibrated instrumented tweezers, like those we employed in this study, operators can be trained to apply controlled forces during optic nerve crush to produce consistent and predictable post-crush cell death. The data and knowledge gathered from this study could aid the design and development of a new instrument with geometry and functionality tailored for optic nerve crush experiments to induce consistent damage to the optic nerve with controlled force, duration, and location.

Figure Legends

Figure 1. The prototype of a cross-action Dumont #N7 tweezers instrumented with miniature precision foil strain gauges and packaged to protect against damage due to mechanical handling.

Figure 2. Cross sections of control and crushed optic nerves. Each dark circle represents one axon immunostained by PPD(1:50, Fisher) . After optic nerve crush, the axon exhibited degenerative signs such as decreased axon density, widespread vacuole accumulation (orange arrow), axon swelling (green arrows), and prevalence of degenerative debris such as the dystrophic neurites (blue arrows). Scale bars: 100 µm (top) and 50 µm (bottom).

Figure 3. The plot of axon density of a post-crush optic nerve plotted against the force impulse (newton-second). The resulting curve indicates that prolonged optic nerve crush and increased force of that crush will lead to decreased axon density at 3-days post-crush. AD: axon density; FI: force impulse.

Figure 4. Plot of force and duration of the optic nerve crush injury delivered by the self-closing tweezers. The data shows no correlation between the time of the crush and the intensity.

Acknowledgements

R01EY026286 (XL), R01EY029121 (XL), and NSF 0938072 (LS).

References

Burke W, Burne JA, Martin PR. 1985. Selective block of Y optic nerve fibres in the cat and the occurrence of inhibition in the lateral geniculate nucleus. *The Journal of physiology* 364: 81-92

Chen H, Zhao Y, Liu M, Feng L, Puyang Z, et al.. 2015. Progressive degeneration of retinal and superior collicular functions in mice with sustained ocular hypertension. *Investigative ophthalmology & visual science* 56: 1971-84

Cone FE, Steinhart MR, Oglesby EN, Kalesnykas G, Pease ME, Quigley HA. 2012. The effects of anesthesia, mouse strain and age on intraocular pressure and an improved murine model of experimental glaucoma. *Experimental eye research* 99: 27-35

Cottee LJ, FitzGibbon T, Westland K, Burke W. 1991. Long Survival of Retinal Ganglion Cells in the Cat After Selective Crush of the Optic Nerve. *Eur J Neurosci* 3: 1245-54

Duan X, Qiao M, Bei F, Kim IJ, He Z, Sanes JR. 2015. Subtype-specific regeneration of retinal ganglion cells following axotomy: effects of osteopontin and mTOR signaling. *Neuron* 85: 1244-56

Feng DF, Chen ET, Li XY, Liu Y, Wang Y. 2010. Standardizing optic nerve crushes with an aneurysm clip. *Neurol Res* 32: 476-81

Fischer D, Harvey AR, Pernet V, Lemmon VP, Park KK. 2017. Optic nerve regeneration in mammals: Regenerated or spared axons? *Exp Neurol* 296: 83-88

Gellrich NC, Schimming R, Zerfowski M, Eysel UT. 2002. Quantification of histological changes after calibrated crush of the intraorbital optic nerve in rats. *Br J Ophthalmol* 86: 233-7

Howell GR, Libby RT, Jakobs TC, Smith RS, Phalan FC, et al.. 2007. Axons of retinal ganglion cells are insulted in the optic nerve early in DBA/2J glaucoma. *The Journal of cell biology* 179: 1523-37

Howell GR, Libby RT, John SW. 2008. Mouse genetic models: an ideal system for understanding glaucomatous neurodegeneration and neuroprotection. *Prog Brain Res* 173: 303-21

Huang HB, Zhang YX, Zhang SH, Ma ZZ. 2015. Calibration and standardisation of graded optic nerve injuries in rats. *Neurol Res* 37: 638-49

Huang ZJ, Kirkwood A, Pizzorusso T, Porciatti V, Morales B, et al.. 1999. BDNF regulates the maturation of inhibition and the critical period of plasticity in mouse visual cortex. *Cell* 98: 739-55

Kalesnykas G, Oglesby EN, Zack DJ, Cone FE, Steinhart MR, et al.. 2012. Retinal ganglion cell morphology after optic nerve crush and experimental glaucoma. *Investigative ophthalmology & visual science* 53: 3847-57

Klocker N, Zerfowski M, Gellrich NC, Bahr M. 2001. Morphological and functional analysis of an incomplete CNS fiber tract lesion: graded crush of the rat optic nerve. *J Neurosci Methods* 110: 147-53

Leung CK, Lindsey JD, Crowston JG, Lijia C, Chiang S, Weinreb RN. 2008. Longitudinal profile of retinal ganglion cell damage after optic nerve crush with blue-light confocal scanning laser ophthalmoscopy. *Investigative ophthalmology & visual science* 49: 4898-902

Li Y, Schlamp CL, Nickells RW. 1999. Experimental induction of retinal ganglion cell death in adult mice. *Investigative ophthalmology & visual science* 40: 1004-8

Li Y, Semaan SJ, Schlamp CL, Nickells RW. 2007. Dominant inheritance of retinal ganglion cell resistance to optic nerve crush in mice. *BMC Neurosci* 8: 19

Libby RT, Li Y, Savinova OV, Barter J, Smith RS, et al.. 2005. Susceptibility to neurodegeneration in a glaucoma is modified by Bax gene dosage. *PLoS Genet* 1: 17-26

Maeda K, Sawada A, Matsubara M, Nakai Y, Hara A, Yamamoto T. 2004. A novel neuroprotectant against retinal ganglion cell damage in a glaucoma model and an optic nerve crush model in the rat. *Investigative ophthalmology & visual science* 45: 851-6

May CA, Lutjen-Drecoll E. 2002. Morphology of the murine optic nerve. *Investigative ophthalmology & visual science* 43: 2206-12

Nickells RW, Howell GR, Soto I, John SW. 2012. Under pressure: cellular and molecular responses during glaucoma, a common neurodegeneration with axonopathy. *Annual review of neuroscience* 35: 153-79

Oglesby E, Quigley HA, Zack DJ, Cone FE, Steinhart MR, et al.. 2012. Semi-automated, quantitative analysis of retinal ganglion cell morphology in mice selectively expressing yellow fluorescent protein. *Experimental eye research* 96: 107-15

Puyang Z, Feng L, Chen H, Liang P, Troy J, Liu X. 2016. Retinal Ganglion Cell Loss is Delayed Following Optic Nerve Crush in NLRP3 Knockout Mice. *Scientific Reports* 6: 20998

Puyang Z, Gong HQ, He SG, Troy JB, Liu X, Liang PJ. 2017. Different functional susceptibilities of mouse retinal ganglion cell subtypes to optic nerve crush injury. *Experimental eye research* 162: 97-103

Quigley HA. 2016. Understanding Glaucomatous Optic Neuropathy: The Synergy Between Clinical Observation and Investigation. *Annu Rev Vis Sci* 2: 235-54

Quigley HA, Addicks EM, Green WR, Maumenee AE. 1981. Optic nerve damage in human glaucoma. II. The site of injury and susceptibility to damage. *Arch Ophthalmol* 99: 635-49

Sarikcioglu L, Demir N, Demirtop A. 2007. A standardized method to create optic nerve crush: Yasargil aneurysm clip. *Experimental eye research* 84: 373-7

Sharma TP, McDowell CM, Liu Y, Wagner AH, Thole D, et al.. 2014. Optic nerve crush induces spatial and temporal gene expression patterns in retina and optic nerve of BALB/cJ mice. *Mol Neurodegener* 9: 14

Tang AD, Makowiecki K, Bartlett C, Rodger J. 2015. Low intensity repetitive transcranial magnetic stimulation does not induce cell survival or regeneration in a mouse optic nerve crush model. *PloS one* 10: e0126949

Templeton G. 2012. A practical approach to optic nerve crush in the mouse. *Mol Vis* 18: 2147–52

Tsai RK, Chang CH, Wang HZ. 2008. Neuroprotective effects of recombinant human granulocyte colony-stimulating factor (G-CSF) in neurodegeneration after optic nerve crush in rats. *Experimental eye research* 87: 242-50

Figures

Figure 1

Figure 2

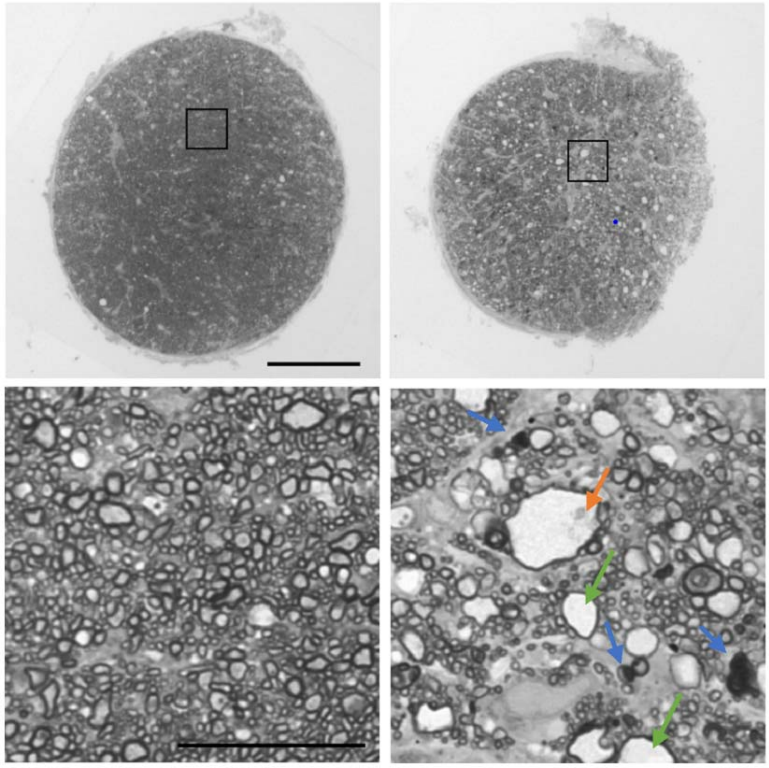

Figure 3

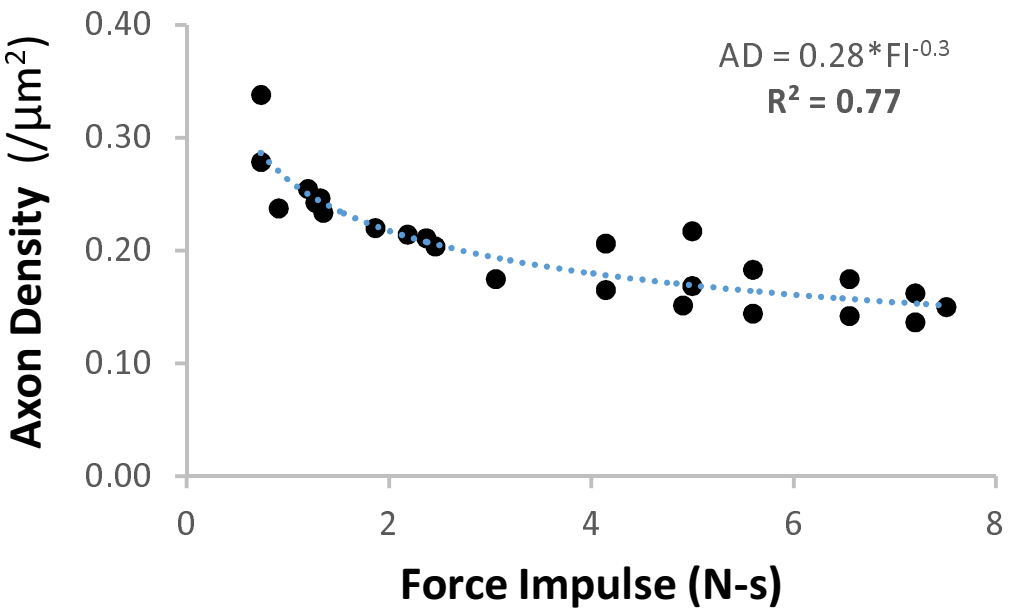

Figure 4

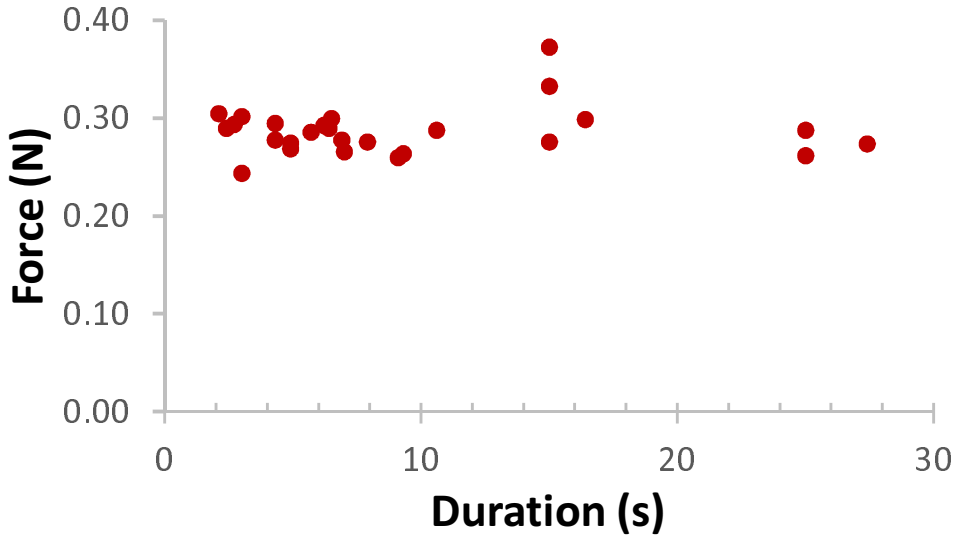

Table 1. Comparison of crush setups and corresponding RGC loss

Studies	Crush Parameters			RGC Loss							Imaging Method
	Position (post. to globe)	Forceps (self-closing)	Duration	1d	4d	1w	9d	2w	3w	1m	
(Leung et al. 2008)	1mm	Dumont #5	2-3 s			82% (±2.3%) SD		89% (±3.4%) SD	92% (±5.3%) SD		*in vivo*, Thy1-CFP
(Libby et al. 2005)	0.5mm	Jeweler's Forceps	4 s						40% (±5.3%) SD		Nissl Stain Cresyl-violet
(Li et al. 1999)	0.5mm	Dumont #7	3 s						58% (±8.1%) SD		Nissl Stain
(Cone et al. 2012)	---	Surgical Forceps	3 s	27% (±12%) SD	42% (±7%) SD		64% (±10%) SD				Thy1-YFP confocal
(Templeton 2012)	1-3mm	Dumont #7	10 s							55% (±13%) SEM	TO-PRO3 confocal
(Sharma et al. 2014)	0.5mm	Jeweler's Forceps	4 s			10% (±10%) SD		30% (±20%) SD		50% (±5%) SD	*in vitro* Cresyl-violet
(Huang et al. 1999)	3mm	Surgical Forceps	---							56%	Neurobiotin Fluor. scope
(Duan et al. 2015)	1mm	Dumont #5	5 s					20% (±4%) SD			Transgenic markers confocal
(Puyang et al. 2016)	1mm	Dumont #7	3 s			45% (±4%) SEM		65% (±3%) SEM	85% (±3%) SD		*in vivo* Thy1-YFP

Table Legend. The most common tools employed for optic nerve crush (ONC) are surgical tweezers. The optic nerve is pinched for 2-10 seconds and the degree of RGC loss varies substantially from laboratory to laboratory.